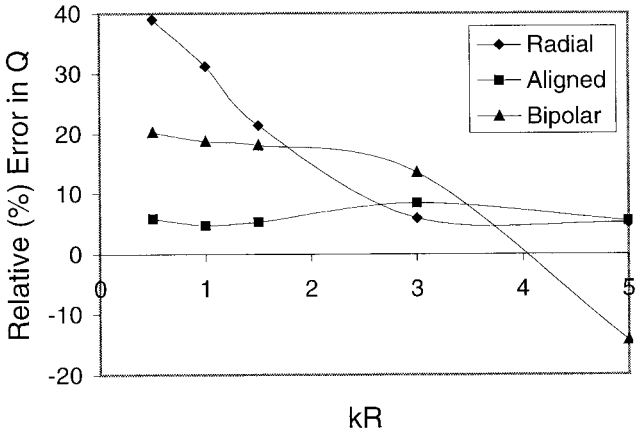

Figure 4 Relative error in the scattering efficiency factor Q versus kR, calculated for PDLC spherical droplets with radial, aligned, and bipolar configurations

eventually grow higher if we continue increasing kR and move beyond any validity of the RG approximation (as in Figure 2). It is inferred from Figure 4 that bipolar droplets also show a similar error variation, with higher errors encountered closer to $kR = 0.5$ and an error null close to $kR = 4$. On the other hand, aligned droplets more closely resemble the isotropic sphere case and manifest a weak oscillatory behaviour in their average error. The stronger error found in radial and bipolar droplets might be attributed to their inhomogeneous structure ($\partial\tilde{\varepsilon}/\partial r \neq 0$) as opposed to the aligned anisotropic or isotropic spherical counterparts.

4. CONCLUSION

For PDLC droplets in the range $0.5 \leq kR \leq 5$ it was found that the RG method provides a correct general estimate to the variation of the differential scattering cross section for the analysed types of droplet configuration. As no analytical solution is available, the FDTD method combined with a very fine grid was used to provide an accurate numerical calculation for the differential cross section. Typical local and average errors for the RG method in the above range are usually around 10–20%. However, higher errors have also been recorded, in particular for radial droplets where average errors of around 40% were found. A rather surprising behaviour for the error variation is noticed: error is not a monotonic increasing function for increased values of kR in the above range. It is found that in some cases the error for kR close to 0.5 is significantly higher to the error occurring when kR is close to 3 or 4, contrary to the intuitive expectation that smaller values of kR should lead to reduced errors. This unexpected error behaviour has also been observed in the particular case of radial droplets when the RG method was assessed against the DDA.

REFERENCES

1. G.P. Crawford and S. Zumer (Eds.), Liquid crystals in complex geometries, Taylor and Francis, London, 1996.
2. P.J. Collings and J.S. Patel (Eds.), Handbook of liquid crystal research, Oxford University Press, Oxford, 1997, Ch. 9.
3. S.J. Slosowicz and J. Zmija, Optics and electro-optics of polymer-dispersed liquid crystals: Physics, technology and application, Optical Eng 34 (1995), 3440–3450.
4. S.J. Cox, V.Y. Reshetnyak, and T.J. Sluckin, Effective medium theory of light scattering in polymer dispersed liquid crystal films, J Phys D: Appl Phys 31 (1998), 1611–1625.
5. J.R. Kelly and W. Wu, Multiple scattering effects in polymer dispersed liquid crystals, Liquid Crystals 14 (1993), 1683–1694.
6. S. Zumer and J.W. Doane, Light scattering from a small nematic droplet, Phys Rev A 34 (1986), 3373–3385.
7. S. Zumer, Light scattering from nematic droplets: Anomalous diffraction approach, Phys Rev A 37 (1988), 4006–4015.
8. E.E. Kriezis and S.J. Elston, Light wave propagation in liquid crystal displays by the 2-D finite-difference time-domain method, Optics Comm 177 (2000), 69–77.
9. E.E. Kriezis, C.J. Newton, T.P. Spiller, and S.J. Elston, 3-D simulations of light propagation in periodic liquid crystal microstructures, Applied Optics (2002), in press.
10. A. Ishimaru, Electromagnetic wave propagation, radiation and scattering, Prentice Hall, New Jersey, 1991.
11. C.F. Bohren and D.R. Hoffman, Absorption and scattering of light by small particles, Wiley, New York, 1983.
12. A. Taflove and S.C. Hagness, Computational electrodynamics: The finite-difference time-domain method, Artech House, Boston, 2000.
13. C.A. Balanis, Advanced engineering electromagnetics, Wiley, New York, 1989.
14. V.A. Lioko and V.I. Molochko, Polymer-dispersed liquid crystal droplets: Calculations of light scattering, Mol Cryst Liq Cryst 331 (1999), 541–548.
15. B.T. Draine and P.J. Flatau, Discrete-dipole approximation for scattering calculations, J Opt Soc Am A 11 (1994), 1491–1499.

FIBER-RING LASER-BASED FIBER GRATING SENSOR SYSTEM USING SELF-HEALING RING ARCHITECTURE

Peng-Chun Peng, Hong-Yih Tseng, and Sien Chi
Institute of Electro-Optical Engineering
National Chiao-Tung University
Hsinchu, Taiwan, 300, R.O.C.

Received 12 June 2002

ABSTRACT: *This paper presents a self-healing fiber grating sensor system and demonstrates its effectiveness. The self-healing function is constructed by using a primary ring architecture incorporated with several ring sub-networks. To enhance the sensing signal when a breakpoint suddenly occurs in the network, we employ a fiber-ring laser-based sensor system. The network survivability of an 11-point FBG sensor is experimentally examined. The proposed fiber grating sensor system can increase the reliability of a sensing network.* © 2002 Wiley Periodicals, Inc. Microwave Opt Technol Lett 35: 441–444, 2002; Published online in Wiley InterScience (www.interscience.wiley.com). DOI 10.1002/mop.10633

Key words: *fiber sensor; fiber Bragg grating; self-healing ring architectures; fiber laser*

1. INTRODUCTION

Fiber Bragg grating (FBG) sensors for distributed sensing in smart structure applications have attracted interest [1]. A FBG sensor system with 60 sensors has been experimentally demonstrated, using a combination of wavelength division multiplexing (WDM) and time division multiplexing (TDM) [2]. Other FBG multiplexing techniques developed include code division multiplexing access (CDMA) [3] and intensity and wavelength division multiplexing (IWDM) [4]. Large-scale FBG sensor systems can be established according to these multiplexing schemes or their combinations. Therefore, enhancing the reliability of FBG sensor systems is very important. However, the in-line topology or tree topology generally adopted in a fiber sensor system cannot protect

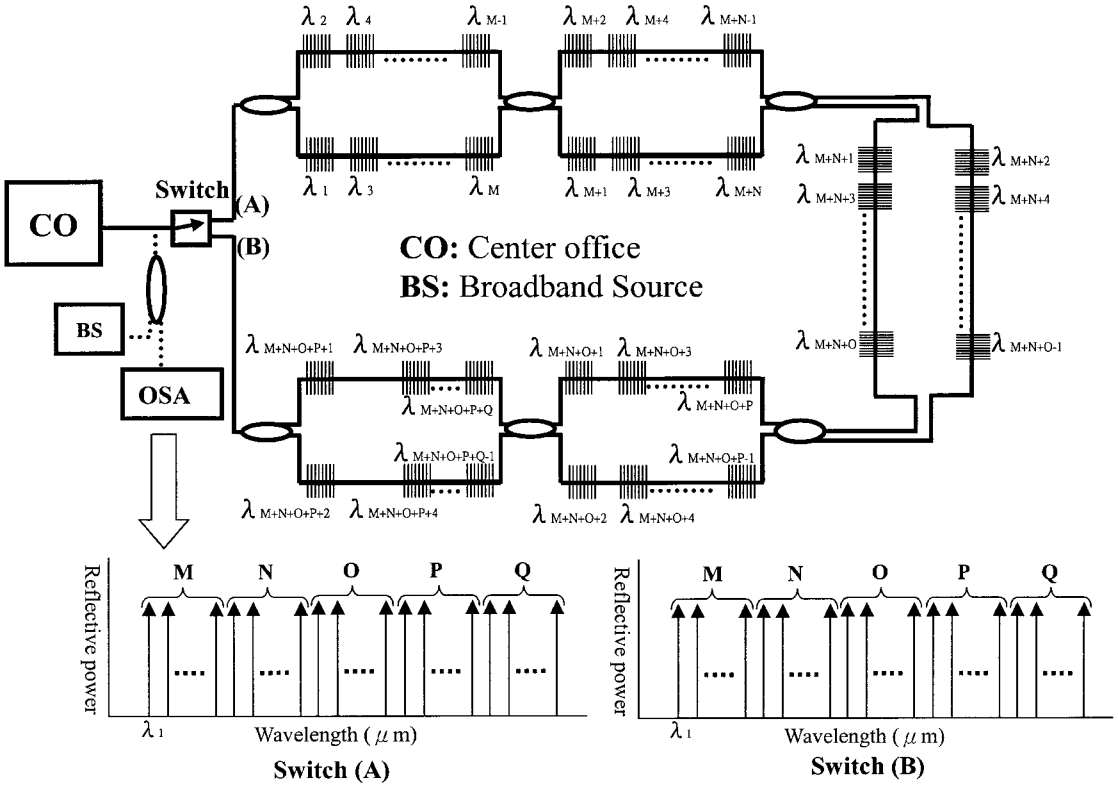

Figure 1 FBG sensor system using self-healing ring architecture

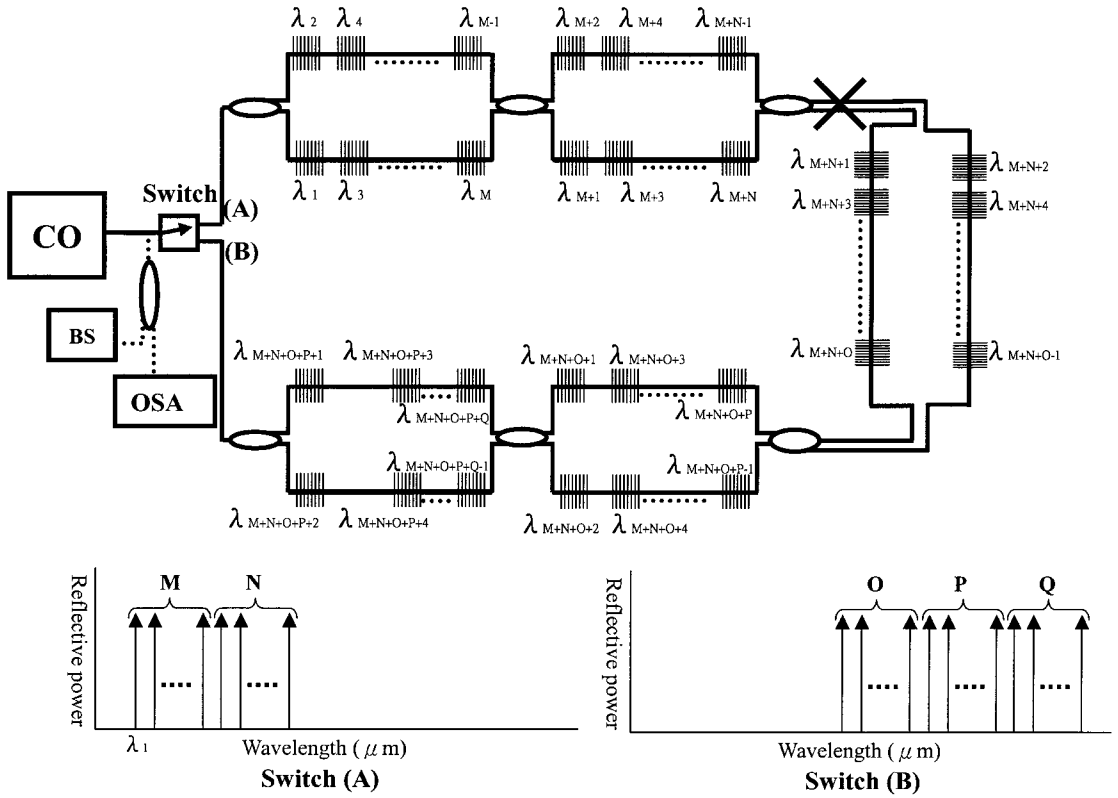

Figure 2 Reconfiguration of an FBG sensor system under link failure in two fibers

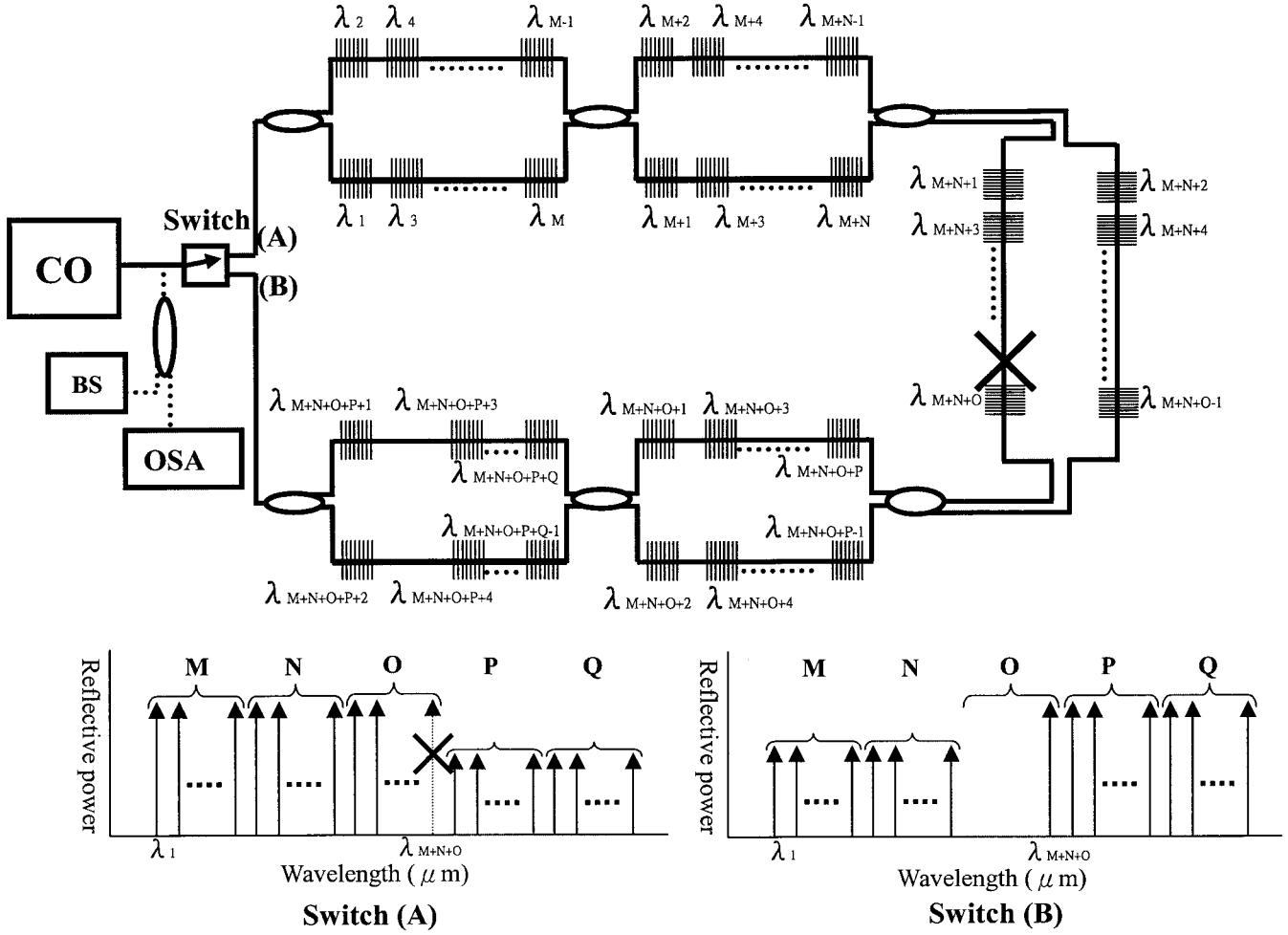

Figure 3 Reconfiguration of an FBG sensor system under link failure in one fiber

the sensing network. Survivability of an FBG sensor network remains a challenge for practical applications.

This paper presents a novel FBG sensor system that uses a self-healing ring architecture to increase the sensing reliability. The self-healing function is constructed by using primary ring architecture incorporated with several ring sub-networks. A 1×2 switch in the ring architecture is used to check the breakpoint in the fiber sensor network. Such a simple self-healing function of this ring topology can support real-time monitoring and reveal the sudden breakpoint of the fiber link. Furthermore, because cutting the fiber in the ring architecture reduces the signal-to-noise ratio (SNR), we adopt a fiber-ring laser-based sensor system. FBG sensor systems based on fiber laser structures have been extensively investigated because of their intense output power, high SNR, and ability to be incorporated with fiber communication systems [5–6]. The FBGs in our proposed sensor network are used as fiber-laser feedback elements. The benefits of a fiber-laser system and self-healing ring architecture can facilitate highly reliable long-distance sensing in a smart structure.

2. PRINCIPLE

Figure 1 schematically shows the proposed FBG sensor system that uses a self-healing ring architecture. The FBG sensor system comprises the sensing FBGs and a center office (CO) that provides the light source and discriminates the reflected signal from FBGs. The light source for the FBG sensor system can be a broadband source (BS). After the broadband source is fed into the FBGs, the backreflected light from the FBGs involves the sensing signal via the reflected wavelength. The wavelength of the sensing FBGs can be monitored by using an optical spectrum analyzer (OSA). The self-healing ring architecture offers survival function under link failure by reconfiguring the fiber network.

Figure 2 depicts two cut fibers in a link. When the switch is in state (A), the FBGs (from λ_{M+N+1} to $\lambda_{M+N+O+P+Q}$) lose their sensing signal. However, the state of switch (B) can be modified to reconfigure the signal of the FBGs (from λ_{M+N+1} to $\lambda_{M+N+O+P+Q}$). Figure 3 shows one fiber cut in a link. When the switch is in state (A), the FBG (λ_{M+N+O}) loses information; moreover, the FBGs (from $\lambda_{M+N+O+1}$ to $\lambda_{M+N+O+P+Q}$) lose 3-dB power. Nevertheless, the switch states at (B) can be modified to reconfigure the FBG (λ_{M+N+O}). However, the 3-dB power loss of FBGs (from $\lambda_{M+N+O+1}$ to $\lambda_{M+N+O+P+Q}$) reduces the SNR in state (A).

In order to reduce the influence of the 3-dB loss on the sensing system, in this paper we use a fiber-ring laser configuration to enhance the SNR. The FBGs in the sensor network are used as fiber-laser feedback elements. The capability of this ring-laser-based sensor system is implemented by tuning a wavelength-selective filter located within the laser cavity for interrogating the Bragg wavelengths of all FBGs. The Bragg wavelength shifts of the sensing FBGs, induced by quasi-static strain or temperature drift, can be detected by the lasing wavelength shifts of the system.

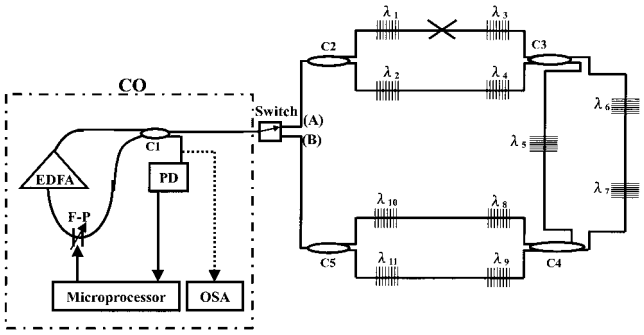

Figure 4 Fiber-ring laser-based fiber Bragg grating sensor system using self-healing ring architecture

3. EXPERIMENT SETUP AND RESULTS

Figure 4 depicts the laser configuration with a tunable Fabry–Perot (FP) filter as a wavelength selection element. It was constructed using an erbium-doped fiber amplifier (EDFA), a 2 × 2 coupler (C1), and the FBGs being used as fiber-laser feedback elements. The lasing light emerging from coupler C1 arrived in a photo detector (PD). This signal was then fed into a microprocessor to calculate the lasing wavelength. The wavelengths λ_i (i = 1, 2, . . . , 11) of the sensing FBGs connected to one end of switch (A) were, from left to right, 1558.11, 1556.46, 1554.42, 1552.47, 1550.43, 1548.39, 1546.74, 1544.25, 1542.93, 1540.14, and 1538.13 nm and the reflectivities were all approximately 99%. Laser output coupling was provided by one port of coupler C1. With sufficient pump power, the system lases once the transmitted wavelength of the filter equals the wavelength reflected from the sensing grating. Thus, the lasing wavelength of the system can be used to accurately measure quasi-static strain or thermal perturbation imposed on the FBGs. When the fiber link fails in one of the fibers, the filter is tuned by using a controller to select the transmitted wavelength over a working range from 1535 nm to 1570 nm. The tuned wavelengths were set at the ten wavelengths of the sensing FBGs (λ_i; i = 1, 2, 4, 5, 6, 7, 8, 9, 10, 11), as shown in Figure 5. The FBG (λ_3) loses its signal. Nevertheless, the state of switch (B) can be modified to reconfigure the FBG (λ_3), as

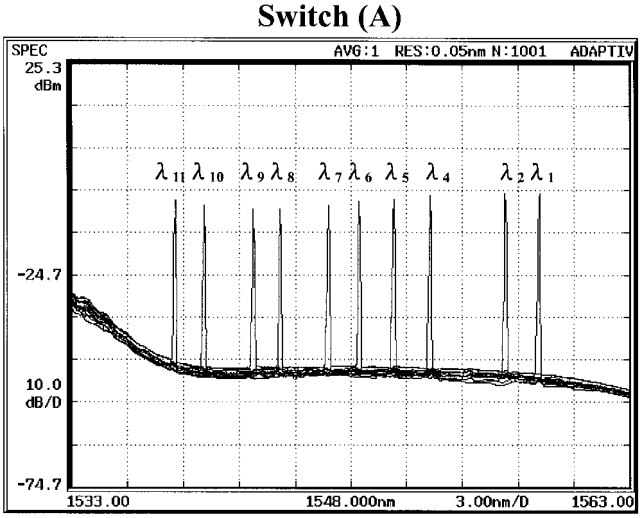

Figure 5 Fiber-laser spectra at various tuned wavelengths; when the fiber link fails in one of the fibers, the FBG (λ_3) loses its signal

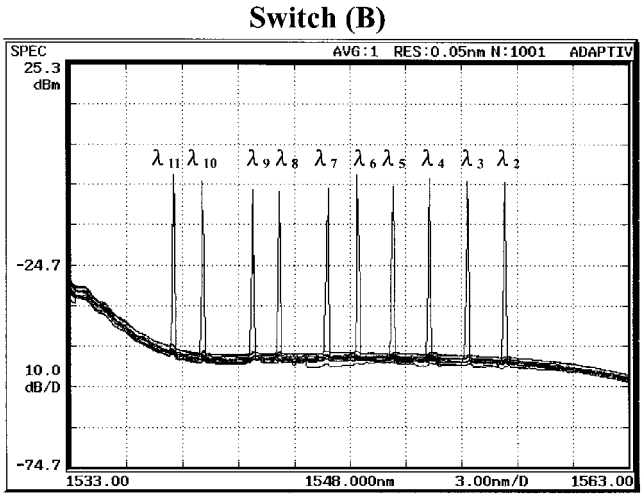

Figure 6 Fiber-laser spectra at various tuned wavelengths; the self-healing ring architecture can regenerate the sensing signal of the FBG (λ_3)

shown in Figure 6. Consequently, the self-healing ring architecture can regenerate the sensing signal of the FBG (λ_3).

4. CONCLUSION

This paper describes a novel self-healing fiber grating sensor system and demonstrates its effectiveness. The network survivability of this proposed FBG sensor is examined by adding a switch in the primary ring architecture incorporated with several ring sub-networks. The experiment involved an 11-point sensor system. Experimental results showed that the tunable multiport fiber laser for WDM enhances the SNR, resolution, and reliability of the sensor system.

ACKNOWLEDGMENT

This work was supported by the Academic Excellence Program of the R.O.C. Ministry of Education under Contract 90-E-FA06-1-4-90X023.

REFERENCES

1. A.D. Kersey, M.A. Davis, H.J. Partrick, M. Leblance, K.P. Koo, C.G. Askins, M.A. Putnam, and E.J. Friebele, Fiber grating sensors, J Lightwave Technol 15 (1997), 1442–1463.
2. M.A. Davis, D.G. Bellemore, M.A. Putnam, and A.D. Kersey, Interrogation of 60 fiber Bragg grating sensors with microstrain resolution capability, Electron Lett 32 (1996), 1393–1394.
3. K.P. Koo, A.B. Tveten, and S.T. Vohra, Dense wavelength division multiplexing of fibre Bragg grating sensors using CDMA, Electron Lett 35 (1999), 165–167.
4. L. Zhang, Y. Liu, J.A.R. Wiliams, and I. Bennion, Enhanced FBG strain sensing multiplexing capacity using combination of intensity and wavelength dual-coding technique, IEEE Photon Technol Lett 11 (1999), 1638–1641.
5. S. Kim, J. Kwon, S. Kim, and B. Lee, Multiplexed strain sensor using fiber grating-tuned fiber laser with a semiconductor optical amplifier, IEEE Photon Technol Lett 13 (2001), 350–351.
6. Talaverano, S. Abad, S. Jarabo, M. Lopez-Amo, Multiwavelength fiber laser sources with Bragg-grating sensor multiplexing capability, J Lightwave Technol 19 (2001), 553–558.